Solvent effect on the sensitized photooxygenation of cyclic and acyclic α-diimines

Else Lemp,* Antonio L. Zanocco, German Günther and Nancy Pizarro

Universidad de Chile, Facultad de Ciencias Químicas y Farmacéuticas, Departamento de Química Orgánica y Fisicoquímica, Casilla 233, Santiago-1, Santiago, Chile

Abstract—The reaction of singlet molecular oxygen with a series of cyclic and acyclic α-diimines was studied. Time-resolved methods were used to measure total reaction rate constants and steady-state methods were used to determine chemical reaction rate constants. GC–MS was used to tentatively assign the reaction products. 5,6-Disubstituted cyclic α-diimines are singlet oxygen quenchers, but become more effective in polar solvents. A reaction mechanism involving a perepoxide intermediate or transition state leading to a hydroperoxide seems to be a key reaction path for product formation. A replacement of the phenyl substituent for a methyl substituent opens up an additional reaction involving a perepoxide-like exciplex, which increases singlet oxygen quenching of the cyclic α-diimines. The reactivity of 5,6-disubstituted cyclic α-diimines towards singlet oxygen is highly dependent on steric interactions arising from vicinal phenyl rings and from electronic effects. 1,4-Disubstituted acyclic α-diimines are, by comparison, moderate or poor singlet oxygen quenchers. Total rate constants are scarcely dependent on solvent properties, but instead correlate with the Hildebrand parameter. These results are explained in terms of a mechanism involving a dioxetane-like exciplex that gives rise to a charged intermediate leading to products.

1. Introduction

The interaction of singlet oxygen ($O_2(^1\Delta_g)$) with a target molecule (Q) involves physical (deactivation) and/or chemical (reactive) processes. This process can be represented in Eqs. 1–3

$$^1O_2 \xrightarrow{k_d} O_2 \quad (1)$$

$$^1O_2 + Q \xrightarrow{k_Q} Q + O_2 \quad (2)$$

$$^1O_2 + Q \xrightarrow{k_R} \text{products} \quad (3)$$

where k_d is the solvent dependent decay rate of singlet oxygen that determines its unperturbed lifetime ($\tau_o=1/k_d$), k_Q corresponds to a second-order rate constant of physical deactivation and k_R is the second-order rate constant of the reactive pathway. Measurement of the lifetime of singlet oxygen at different concentrations of Q permits one to obtain a k_T value, where $k_T=k_Q+k_R$. Evaluation of k_R requires the measurement of quantum yields of oxygen consumption and/or product formation, where these values can be difficult to obtain. Values of k_Q and k_R can be solvent dependent, where solvent may modify each to a similar extent, thus keeping k_R/k_T constant. Such a similar behaviour can then be ascribed to an analogous mechanism and/or a common transition state. However, differences in the solvent effect between k_Q and k_R would suggest dissimilar transition states for each process. For example, a reaction containing different intermediates or different pathways may still follow from a common intermediate. Thus, the analysis of solvent effect on k_T and/or k_R provides valuable information regarding the nature of the reaction process. Many singlet oxygen reaction rate constants measured before 1999 have been compiled by Wilkinson et al.[1] Solvent effects on singlet oxygen reactions have been reviewed,[2–6] where rate constant differences have been correlated with solvent dielectric constants,[7–9] solvent hydrogen bonding (with the target molecule),[10] and/or hydrophobic interactions.[11] In the last decade, linear solvation energy relationships (LSER) and theoretical linear solvation energy relationships (TLSER) have been employed to interpret singlet oxygen reaction mechanisms with amine,[5,12–16] polycyclic aromatic compounds,[11] furan,[17] alkaloids[5,18,19] and biologically active (polyfunctional) compounds.[14,17,18,20,21] Such LSER treatments allow a quantitative evaluation of solvent effect in terms of different descriptors. The relative contribution of each descriptor included in the correlation equation depends on the substrate. Common features are observed for compounds belonging to the same family reacting through the same mechanism.

* Corresponding author. Tel.: +56 2 9782877; fax: +56 2 9782868; e-mail: elemp@ciq.uchile.cl

The determination of a model compound correlation equation permits to calibrate and validate the linear free energy relationship in a given solvent set, giving a basis for predictions to the behaviour in other solvents. The formalism may be used to determine the main reaction site in polyfunctional compounds, to detect changes in the reaction mechanism with solvent properties, and to evaluate the relative contribution of tautomers in equilibrium to the total reaction rate. Also, the analysis could be extended to singlet oxygen reactivity in microheterogeneous systems to predict relative rate constants in such systems. However, when using this formalism, several limitations should be considered. First, this type of multilinear correlation is based on the assumption that the various descriptors are orthogonal, i.e., for a given parameter there is no cross-correlation with the other. Second, the barely reproducible rate constant values reported by different laboratories must be carefully stated to improve data reproducibility, which depends on various experimental critical points—e.g., sensitizer stability and reactivity, solvent purity, time of reaction and substrate consumption fraction in steady-state experiments, laser power and number of accumulated shots in time-resolved techniques.

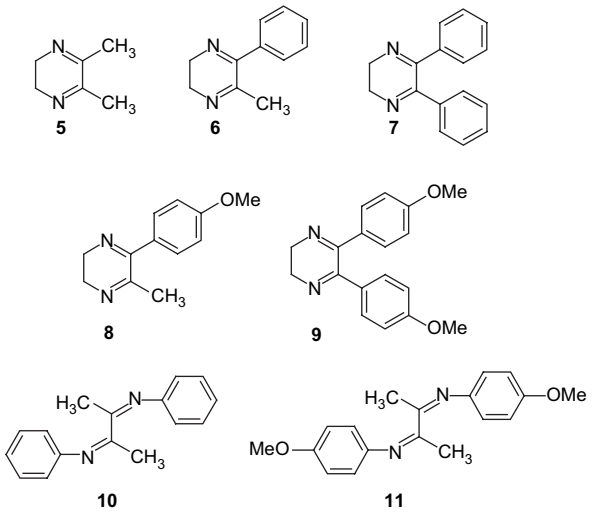

Figure 1. Structures of cyclic α-diimines: 5,6-dimethyl-2,3-dihydropyrazine (**5**), 5-methyl-6-phenyl-2,3-dihydropyrazine (**6**), 5,6-diphenyl-2,3-dihydropyrazine (**7**), 5-methyl-6-(*p*-methoxyphenyl)-2,3-dihydropyrazine (**8**), 5,6-bis(*p*-methoxyphenyl)-2,3-dihydropyrazine (**9**), and acyclic α-diimines: 1,4-diaza-1,4-diphenyl-2,3-dimethyl-1,3-butadiene (**10**), 1,4-diaza-1,4-bis(*p*-methoxyphenyl)-2,3-dimethyl-1,3-butadiene (**11**).

A large number of studies have focused on reactions of singlet oxygen with molecules containing C=C double bonds. On the contrary, little data is available on reactions of singlet oxygen with molecules containing C=N double bonds.[22–26] A product distribution may depend on temperature and substituents in reactions of $O_2(^1\Delta_g)$ with imino compounds and may involve several intermediates (Scheme 1), i.e., dioxazetidines (**1**) from [2+2] concerted cycloaddition to the carbon–nitrogen double bond;[23,24] peroxide ions (**2**) from electrophilic attack on iminic carbon[23] and hydroperoxides (**4**) from rearrangement of pernitrones (**3**) in reactions with substituted 2,3-dihydropyrazines.[27] The involvement of a pernitrone intermediate (**3**) may arise by the interaction of $^1O_2$ with the imine nitrogen lone pair.

Previous studies do not permit one to conclude whether the reaction of singlet oxygen and the imino group is similar to homologous alkenes or whether it departs significantly from this chemistry due to the presence of the nitrogen atom. In previous works,[28] we reported the total rate constant values, k_T, and the chemical reaction rate constant values, k_R, for the reactions between two 5,6-disubstituted-2,3-dihydropyrazines and singlet oxygen in various solvents. Chemical reaction rate constants, k_R, for 5,6-dimethyl-2,3-dihydropyrazine (**5**) were very close to k_T in polar solvents such as propylencarbonate, whereas the contribution of the chemical channel to the total reaction is very low for methyl and phenyl derivatives. Analysis of solvent effect on k_T for the dimethyl derivatives using the semiempirical solvatochromic equation (LSER) of Taft, Kamlet et al.,[29,30] reveals a dependence on the solvent microscopic parameters α and π^*. When the phenyl group is replaced with a methyl group, the dihydropyrazine ring reactivity increases towards singlet oxygen and modifies the dependence of k_T on solvent parameters. The importance with the Hildebrand parameter is apparent.

In the present work, we study reactions of singlet oxygen with cyclic and acyclic α-diimines that possess different substituents on the iminic carbon (Fig. 1). Our aim is to understand the reaction mechanism based on product distributions and kinetics, which includes measurements of rate constants for chemical and physical reaction channels in several solvents. Solvent effects are analyzed in terms of linear solvation energy relationships (LSER).[29–31] LSER relations are

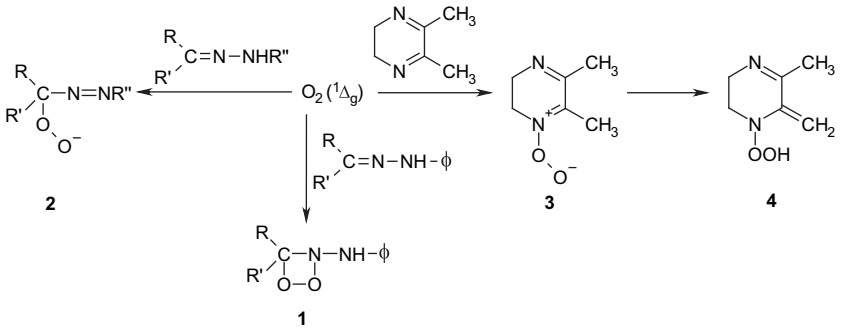

Scheme 1.

of great value in interpreting mechanisms of singlet oxygen reactions since they may permit a quantitative explanation of solvent effects.[5]

2. Results

2.1. Total reaction of singlet oxygen with cyclic α-diimines

The total quenching rate constant (physical and chemical), k_T, for reaction of $O_2(^1\Delta_g)$ with the 5,6-disubstituted-2,3-dihydropyrazines (Fig. 1) in several solvents was obtained from the first-order decay of $O_2(^1\Delta_g)$ in the absence (τ_o^{-1}) and the presence of dihydropyrazine (τ^{-1}) according to Eq. 4.

$$\tau^{-1} = \tau_o^{-1} + k_T[\text{dihydropyrazine}] \quad (4)$$

Linear plots of τ^{-1} vs [dihydropyrazine] were obtained for all solvents employed (Fig. 2). Intercepts of these plots match closely with those reported[20] and measured (in a large number of experiments from our laboratory) for singlet oxygen lifetimes in the identical solvents. Values of k_T calculated from slopes of these plots are given in Table 1. The k_T values were independent of the laser pulse energy (between 2 and 5 mJ) allowing us to disregard secondary processes involving $O_2(^1\Delta_g)$. Singlet oxygen decays after dye laser excitation at 532 nm, with Rose Bengal as sensitizer in acetone, in the absence and the presence of 5,6-dimethyl-2,3-dihydropyrazine (**5**) are shown in the inset of Figure 2. As can be observed, both traces have nearly the same amplitude, indicating that the excited states of the sensitizer were not deactivated by the addition of **5** at the concentrations employed to quench $O_2(^1\Delta_g)$. The same behaviour was observed with TPP—the sensitizer employed in most solvents—in the presence of the different dihydropyrazines studied. The same k_T values were obtained for some solvents (data not shown) either by using competitive steady-state methods, such as the inhibition of the autoxidation rate of rubrene (λ_{max}=520 nm)[32] or by following the

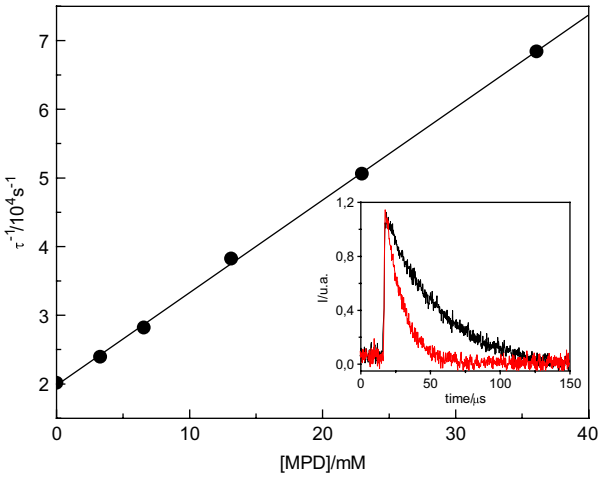

Figure 2. Stern–Volmer plot for deactivation of singlet oxygen by DMD in acetone. Inset (a) Singlet oxygen phosphorescence decay at 1270 nm, following dye laser excitation at 532 nm, with Rose Bengal as sensitizer in acetone. (b) as (a), but with 13.6 mM DMD.

consumption rate of 9,10-dimethylanthracene in the absence and the presence of dihydropyrazine derivatives.[18] Thus, possible rapid chemical changes of samples during illumination or interference on $O_2(^1\Delta_g)$ luminescence with the scattered laser light and the tail end of the sensitizer fluorescence[33] can be dismissed.

A solvent dependence is observed in the total quenching rate constants for all reactions of 5,6-disubstituted-2,3-dihydropyrazines with singlet oxygen (Table 1). The largest effect was found for **5**, for which k_T increases by more than 2 orders of magnitude when the solvent was changed from hexafluoro-2-propanol to *N*,*N*-dimethylacetamide. Similar trends were observed for **6**, **7**, **8** and **9**. The total rate constant value increases by more than 1 order of magnitude when the solvent is changed from protic to non-protic solvents, such as trifluoroethanol vs *N*,*N*-dimethylformamide. In addition, in all solvents the total rate constant for **6** was considerably larger than those for the other cyclic α-diimines. Dihydropyrazines exhibit similar results to those reported for dienes.[1] Thus, the reactivity of the compounds towards singlet oxygen depends both on dihydropyrazine structure as well as solvent properties.

However, solvent effects observed here are larger than those for dienes[2] and cannot be associated merely with changes in macroscopic solvent properties due to the existence of specific solute–solvent interactions.[2,5,28] Thus, a deeper rationalization of solvent effects and interactions of singlet oxygen with dihydropyrazines can be obtained from the analysis of the quenching rate constant dependence on microscopic solvent parameters. The semiempirical solvatochromic equation (LSER) of Taft, Kamlet et al.[29–31] (Eq. 5) was employed.

$$\log k = \log k_o + s\pi^* + d\delta + a\alpha + b\beta + h\rho_H^2 \quad (5)$$

In Eq. 5, π^* accounts for polarizability and dipolarity of solvent,[31,34] δ is a correction term for polarizability, α corresponds to the hydrogen bond donor solvent ability, β indicates solvent capability as a hydrogen bond acceptor, and ρ_H is the Hildebrand parameter, a measure of disruption of solvent–solvent interactions in creating a cavity.[35] The constant term $\log k_o$ in Eq. 5 arises from the method of multiple linear regression and does not have a clear-cut physical meaning. For correlation equations independent of the cavity term, the constant term $\log k_o$ is equal to $\log k$ in solvents such as alkanes, in which all the other parameters are near to zero.

The coefficients in the LSER equation (Eq. 5), *s*, *d*, *a*, *b* and *h*, are obtained by a multilinear correlation analysis on k_T dependence with solvent parameters (Table 2). This analysis is supported on purely statistical criteria. Sample size *N*, product correlation coefficient *R*, standard deviation SD, and the Fisher index of equation reliability *F*, indicate the quality of the overall correlation equation. The reliability of each term is indicated by *t*-statistic *t*-stat, and the variance inflation factor VIF. Suitable quality is indicated by large *N*, *F*, and *t*-stat values; small SD values; and *R* and VIF close to one.[36]

Results in Table 2 show that not all descriptors are statistically reliable. Descriptor coefficients accepted in the correlation equation were those having a significance level ≥0.95.

Table 1. Values of k_T for reactions of cyclic α-diimines with $O_2(^1\Delta_g)$ in different solvents

Solvent	$k_T/10^5$ M^{-1} s^{-1}				
	5	**6**	**7**	**8**	**9**
Hexafluoro-2-propanol	0.26±0.01	—	0.28±0.01	—	0.44±0.02
Trifluoroethanol	1.52±0.16	5.74±0.25	1.75±0.08	3.54±0.18	0.87±0.04
Methanol	5.23±0.22	26.4±1.15	10.6±0.50	20.1±0.99	1.67±0.07
Ethanol	3.69±0.19	22.1±0.99	8.98±0.46	13.0±0.66	2.34±0.11
n-Propanol	8.60±0.38	25.5±1.09	7.20±0.32	12.7±0.64	2.83±0.12
n-Butanol	4.94±0.22	—	—	19.1±0.96	3.36±0.18
n-Pentanol	5.44±0.19	—	—	—	3.06±0.17
Benzyl alcohol	4.48±0.21	23.3±0.09	7.56±0.35	12.7±0.67	3.11±0.17
n-Hexane	3.60±0.17	—	—	10.7±0.56	—
n-Heptane	4.31±0.18	28.9±1.15	—	12.1±0.55	—
Chloroform	3.16±0.13	12.0±0.06	3.56±0.21	—	1.67±0.08
Benzene	5.34±0.21	49.5±1.98	5.66±0.29	18.5±0.89	2.78±0.15
Anisole	6.01±0.33	63.0±2.29	11.4±0.33	24.5±1.29	3.36±0.17
Diethyl ether	6.08±0.31	37.7±1.69	9.32±0.41	16.8±0.70	4.81±0.27
Benzonitrile	6.25±0.41	41.9±1.65	8.35±0.31	24.8±1.17	2.97±0.18
Methylene chloride	7.36±0.31	37.1±1.29	4.56±0.24	12.8±0.59	2.50±0.15
Acetonitrile	9.87±0.41	67.3±3.02	7.99±0.32	23.1±1.11	2.83±0.14
Tetrahydrofuran	12.9±0.48	50.6±2.85	11.7±0.51	25.5±1.15	4.63±0.28
Ethyl acetate	13.6±0.58	51.6±2.12	11.1±0.48	32.1±1.70	3.53±0.20
Acetone	13.7±0.43	60.4±2.63	11.2±0.31	31.1±1.59	3.95±0.19
Dioxane	14.6±0.55	60.8±3.00	11.7±0.37	42.7±2.01	2.99±0.17
N,*N*-Dimethylformamide	19.3±0.72	101.0±4.19	23.6±1.08	46.5±2.22	5.93±0.31
Propylencarbonate	20.3±0.89	68.1±3.27	18.4±0.90	45.9±2.30	4.70±0.24
Tributyl phosphate	56.8±2.34	159.0±4.38	12.6±0.65	—	3.03±0.17
N,*N*-dimethylacetamide	58.3±2.61	—	—	—	—

Table 2. LSER correlation equations for the reaction of singlet oxygen with cyclic α-diimines

	$\log k = \log k_o + s\pi^* + d\delta + a\alpha + b\beta + h\rho_H^2$					
5	$\log k_o$	*s*	*D*	*a*	*b*	*h*
Coeff.	5.577	0.629	−0.406	−0.602	0.439	—
±	0.081	0.140	0.102	0.054	0.125	—
t-Stat.	68.802	4.500	−3.964	−11.053	3.507	—
P(2-tail)	<0.0001	0.0002	0.0008	<0.0001	0.0024	—
VIF	—	1.536	1.808	1.006	1.572	—
	N=24, *R*=0.956, SD=0.144, *F*=50.029					
6	$\log k_o$	*s*	*D*	*a*	*b*	*h*
Coeff.	6.395	—	—	−0.692	0.203	0.003
±	0.056	—	—	0.050	0.084	0.001
t-Stat.	114.69	—	—	−13.855	2.430	4.561
P(2-tail)	<0.0001	—	—	<0.0001	0.0291	0.0004
VIF	—	—	—	1.613	1.379	2.088
	N=18, *R*=0.970, SD=0.075, *F*=74.475					
7	$\log k_o$	*s*	*D*	*a*	*b*	*h*
Coeff.	5.426	—	—	−0.596	0.595	0.004
±	0.072	—	—	0.046	0.112	0.001
t-Stat.	75.320	—	—	−12.853	5.299	4.855
P(2-tail)	<0.0001	—	—	<0.0001	<0.0001	0.0002
VIF	—	—	—	1.300	1.449	1.587
	N=19, *R*=0.976, SD=0.101, *F*=99.432					
8	$\log k_o$	*s*	*D*	*a*	*b*	*h*
Coeff.	5.959	—	—	−0.589	0.376	0.003
±	0.065	—	—	0.060	0.093	0.001
t-Stat.	92.242	—	—	−9.873	4.048	4.198
P(2-tail)	<0.0001	—	—	<0.0001	0.0011	0.0008
VIF	—	—	—	1.585	1.402	2.036
	N=19, *R*=0.943, SD=0.094, *F*=40.038					
9	$\log k_o$	*s*	*D*	*a*	*b*	*h*
Coeff.	5.381	—	—	−0.363	0.469	—
±	0.034	—	—	0.029	0.060	—
t-Stat.	159.483	—	—	−12.458	7.803	—
P(2-tail)	<0.0001	—	—	<0.0001	<0.0001	—
VIF	—	—	—	1.000	1.000	—
	N=21, *R*=0.961, SD=0.074, *F*=109.904					

For this reason ρ_H was not included in LSER correlation for **5**. Similarly, equations for **6**, **7**, **8** and **9** were independent of π^* parameter. According to the LSER coefficients in Table 2, k_T values for **5** increase in solvents with larger capacity to stabilize charges and dipoles and decrease in strong HBD solvents.

Furthermore, for other compounds under study, the rate constants increase in HBA solvents with high cohesive energy and decrease in strong HBD solvents, although rate constant for **9** does not depend on the Hildebrand parameter.

2.2. Chemical reaction of $O_2(^1\Delta_g)$ with dihydropyrazines

Irradiation of aerated solutions of **5**, **6** and **8** in the presence of TPP or RB, at the wavelength where only the sensitizer absorbs, decreases the concentration of these dihydropyrazine compounds. Plots of ln [dihydropyrazine] versus t indicate that the photooxidation reaction follows a first-order kinetics, Eq. 6.

$$r = k_R[^1O_2][\text{dihydropyrazine}] = k_{obs}[\text{dihydropyrazine}] \quad (6)$$

A compound of known reactivity towards singlet oxygen, such as dimethylanthracene (DMA) has been employed as actinometer to evaluate the steady-state concentration of $O_2(^1\Delta_g)$. The reactive rate constants for dihydropyrazines can be evaluated from Eq. 7:

$$k_R^{\text{dihydropyrazine}} = k_R^{\text{actinometer}} \frac{k_{obs}^{\text{dihydropyrazine}}}{k_{obs}^{\text{actinometer}}} \quad (7)$$

We previously reported the rate constant values, k_R, for chemical quenching of $O_2(^1\Delta_g)$ by **5** and **6**, in various solvents (for compound **5**, k_R (n-hexane)=0.06×10^5 M^{-1} s^{-1}; k_R (propylencarbonate)=21.0×10^5 M^{-1} s^{-1}; for compound **6**, k_R (benzene)=2.18×10^5 M^{-1} s^{-1}; k_R (propylencarbonate)=1.53×10^5 M^{-1} s^{-1}).[28] For compound **8**, we found values of k_R very close to those obtained for MPD (k_R (benzene)=1.96×10^5 M^{-1} s^{-1}). For **7** and **9**, we found neither substrate consumption nor product formation when monitoring the photosensitized oxidation of these compounds up to 60 h of irradiation—in ethanol or propylencarbonate as solvent—according to gas chromatography with NPD detection. For **9** in acetonitrile as solvent and TPP as sensitizer, we determined a consumption of 4% after 60 h irradiation. With a careful control of experimental conditions (photon flux, temperature and cell geometry) we measured a singlet oxygen steady-state concentration to be equal to $(1.2\pm0.3)\times10^{-10}$ M with DMA as actinometer. This result implies that k_R values for **7** and **9** would be $\leq10^3$ M^{-1} s^{-1}, and the chemical quenching of singlet oxygen is negligible.

Because of the low substrate concentrations employed and the low conversion yields, no attempts were made to isolate reaction products for spectroscopic characterization. Tentative evidence for product distribution was obtained by GC–MS analysis. GC–MS analyses were carried out after irradiation for 6 h, where 0.001 M substrate (~30 to 40% conversion) was used in acetonitrile solution with TPP as sensitizer. Chromatograms were obtained operating the spectrometer in both the positive chemical ionization (CI+) as well as the electron impact (EI+) modes. A chromatogram of **6** shows only three major peaks. Unreacted **6** is the main one. The CI+ and EI+ mass spectra corresponding to peaks with largest retention times indicate that 1-isocyano-2-(benzoylamino)ethane (**6a**) and 1-isocyano-4-phenyl-4-carboxaldehyde-3-aza-3-butene (**6b**) are the probable main products of photooxidation of **6** (Scheme 2). Additionally, in separate experiments in benzene, we confirmed the formation of formaldehyde (**12**) as one of the photooxidation products by comparison with a chromatogram obtained for formaldehyde in benzene. For **5** we found formaldehyde (**12**), 1-isocyano-2-(acylamino)ethane (**5a**) and 1-isocyano-4-carboxaldehyde-3-aza-3-pentene (**5b**) and for **8** we detected formaldehyde (**12**), 1-isocyano-2-(4-methoxybenzoylamino)ethane (**8a**) and 1-isocyano-4-(4-methoxyphenyl)-4-carboxaldehyde-3-aza-3-butene (**8b**) as the probable main reaction products (Scheme 2). These results show that the photooxidation of **5**, **6** and **8** follows the same reaction path.

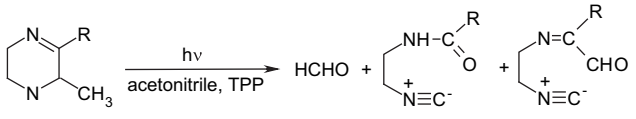

R	X	Y	Z
CH_3	5	5a	5b
ϕ	6	6a	6b
CH_3O-ϕ	8	8a	8b

Scheme 2.

2.3. Total reaction of singlet oxygen with acyclic α-diimines

The total quenching rate constant (physical and chemical), k_T, for reaction of $O_2(^1\Delta_g)$ with acyclic α-diimines (Fig. 1) in several solvents was obtained from the first-order decay of singlet oxygen luminescence as described for cyclic compounds (Eq. 6). The values of k_T obtained from these experiments are summarized in Table 3.

The reactivity of acyclic α-diimines (**10** and **11**) towards singlet oxygen is diminished compared to the cyclic homologous. The total quenching rate constants are 1–2 orders of magnitude smaller compared to those for 5,6-disubstituted-2,3-dihydropyrazines (Table 3).

1,4-Diaza-1,4-bis(*p*-methoxyphenyl)-2,3-dimethyl-1,3-butadiene (**11**) is the more reactive compared to 1,4-diaza-1,4-diphenyl-2,3-dimethyl-1,3-butadiene (**10**) and is strongly solvent dependent with respect to the total rate constant. For **11**, k_T increases by more than 1 order of magnitude when the solvent is changed from trifluoroethanol ($k_T=1.37\pm0.07\times10^5$ M^{-1} s^{-1}) to *N*,*N*-dimethylformamide ($k_T=15.2\pm0.80\times10^5$ M^{-1} s^{-1}). The acyclic α-diimine **10** shows a smaller reactivity with total rate constant values in the order of 10^4 M^{-1} s^{-1} and sparingly solvent dependent. In Table 4 the equation coefficients obtained from the LSER analysis for **11** are included. Our results show that k_T increases in solvents with a larger capacity to stabilize charges and dipoles, high cohesive energy and decrease in strong HBD solvents.

Table 3. Values of k_T for reactions of acyclic α-diimines with $O_2(^1\Delta_g)$ in different solvents

Solvent	$k_T/10^5$ M^{-1} s^{-1}	
	10	**11**
Hexafluoro-2-propanol	0.14±0.01	—
Trifluoroethanol	0.26±0.01	1.37±0.07
Ethanol	0.49±0.02	3.39±0.15
n-Propanol	0.41±0.02	1.69±0.07
n-Butanol	0.48±0.02	2.40±0.13
n-Pentanol	0.35±0.02	2.15±0.12
Acetonitrile	0.16±0.01	10.1±0.49
Acetone	0.12±0.01	8.05±0.38
Ethyl acetate	0.12±0.01	4.71±0.25
N,*N*-Dimethylformamide	0.35±0.02	15.2±0.80
N,*N*-Dimethylacetamide	0.34±0.02	12.5±0.65
Benzene	0.37±0.02	6.48±0.35
n-Hexane	0.17±0.01	1.81±0.10
n-Heptane	0.14±0.01	2.19±0.11
Chloroform	0.42±0.02	3.70±0.17
Dioxane	0.24±0.01	6.25±0.32
Propylencarbonate	0.29±0.01	14.6±0.70
Benzonitrile	0.16±0.01	8.55±0.44
Tetrahydrofuran	0.15±0.01	4.51±0.20
Anisole	0.28±0.01	6.05±0.31
Diethyl ether	0.21±0.01	2.73±0.11

Table 4. LSER correlation equations for the reaction of singlet oxygen with 1,4-diaza-1,4-bis(*p*-methoxyphenyl)-2,3-dimethyl-1,3-butadiene (**11**)

	$\log k = \log k_o + s\pi^* + d\delta + a\alpha + b\beta + h\rho_H^2$					
	$\log k_o$	s	D	a	b	h
Coeff.	5.114	0.592	—	−0.597	—	0.003
±	0.058	0.085	—	0.050	—	0.001
t-Stat.	87.440	6.945	—	−11.867	—	4.746
P(2-tail)	<0.0001	<0.0001	—	<0.0001	—	0.0002
VIF	—	1.647	—	1.553	—	2.208
	N=20, R=0.975, SD=0.079, F=103.392					

In all statistical tests performed for compound **10** including simple linear regression, forward and backward ANOVA test and multiple regression, only we found dependence with the Hildebrand parameter. The correlation shows a coefficient h equal to 0.003, with a regression coefficient between 0.6 and 0.75 (highly dependent on the number of data points considered) and a Fisher index near to 10. Although non-acceptable statistical parameters are found, we believe that the total rate constant for this compound depends primarily on the solvent cohesive energy and the poor correlation is due to the narrow range of k_T values.

2.4. Chemical reaction of singlet oxygen with acyclic α-diimines

Chemical rate constants for reactions of acyclic α-diimines with singlet oxygen were determined in steady-state experiments by irradiating 0.001 M substrate in benzene or propylencarbonate solutions with TPP as the sensitizer. GC-NPD was used to monitor the substrate consumption (up to 30%). In these experiments, 9,10-dimethylanthracene (DMA, k_R (benzene)[37]=2.1×10^7 M^{-1} s^{-1}) was used as the actinometer. The values for k_R calculated with Eq. 7 are summarized in Table 5.

The data in Table 5 show that chemical rate constant increases when solvent is changed from benzene to propylencarbonate. Comparison of k_R values with k_T values shows

Table 5. Chemical reaction rate constants, k_R, for reactions of 1,4-diaza-1,4-diphenyl-2,3-dimethyl-1,3-butadiene (**10**) and 1,4-diaza-1,4-bis(*p*-methoxyphenyl)-2,3-dimethyl-1,3-butadiene (**11**) with $O_2(^1\Delta_g)$ in different solvents

Solvent	$k_R/10^5$ M^{-1} s^{-1}	
	10	**11**
Benzene	0.035±0.002	0.216±0.012
Propylencarbonate	0.0686±0.038	2.120±0.090

that there is a small contribution (in the order of 20%) of the chemical reaction to the total singlet oxygen quenching. The physical quenching is the major deactivation process.

Similar to the dihydropyrazines (low substrate concentration, low conversion yields), we did not attempt to isolate reaction products for spectroscopic characterization, although evidence of product distribution was obtained by GC–MS. For the acyclic α-diimines studied, **10** and **11**, the product distribution was independent of the solvent, but not the relative concentrations. When 0.001 M **11** in benzene was irradiated for 49 h in the presence of TPP, the chromatogram shown in Figure 3a was obtained with the mass spectrometer in the electron impact (EI+) operation mode. Two major peaks are observed, along with two secondary reaction products. Unreacted **11** corresponds to the main peak with a retention time of 22.79 min (Fig. 3b shows the EI+ mass spectrum of **11**).[38] Analyses of the positive chemical ionization (CI+) (not included) and the EI+ mass spectra (Fig. 3e) corresponding to peak with retention time of 25.03 min, indicate that the main photooxidation product in benzene was *N*-(4-methoxyphenyl)-2-[(4-methoxyphenyl)imino]propanamide (**11c**). The peaks at 8.54 and 15.22 min suggest that 1-isocyano-4-methoxybenzene (**11a**) and *N*-(4-methoxyphenyl)acetamide (**11b**) are secondary products of the photooxidation of **11** in benzene (Scheme 3).

Figure 3c and d shows mass spectra ionization patterns and the corresponding proposed structures. In the same way that we previously described, we determined the formation of formaldehyde (**12**) as one of the photooxidation products. The same experiment carried out in propylencarbonate yields 1-isocyano-4-methoxybenzene (**11a**) and *N*-(4-methoxyphenyl)acetamide (**11b**) as main products whereas the product with retention time equal to 25.03 is the minor product. A similar behaviour was observed for **10**. Photooxidation in benzene yields *N*-phenyl-2-(phenylimino)propanamide (**10c**) as the main product. In propylencarbonate, the main reaction products were the 1-isocyano (**10a**) and acetamide derivatives (**10b**).

3. Discussion

3.1. Cyclic α-diimines

The quenching of singlet oxygen by **5** has been discussed earlier by Gollnick et al.[27] Product distribution was explained in terms of a hydroperoxide intermediate resulting from the rearrangement of a primary reaction intermediate, 'pernitrone' or 'nitrone oxide' (**13**) (Scheme 4). Other possible reaction pathways, involving interaction of singlet oxygen with C-5 of the dihydropyrazine to give hydroperoxides

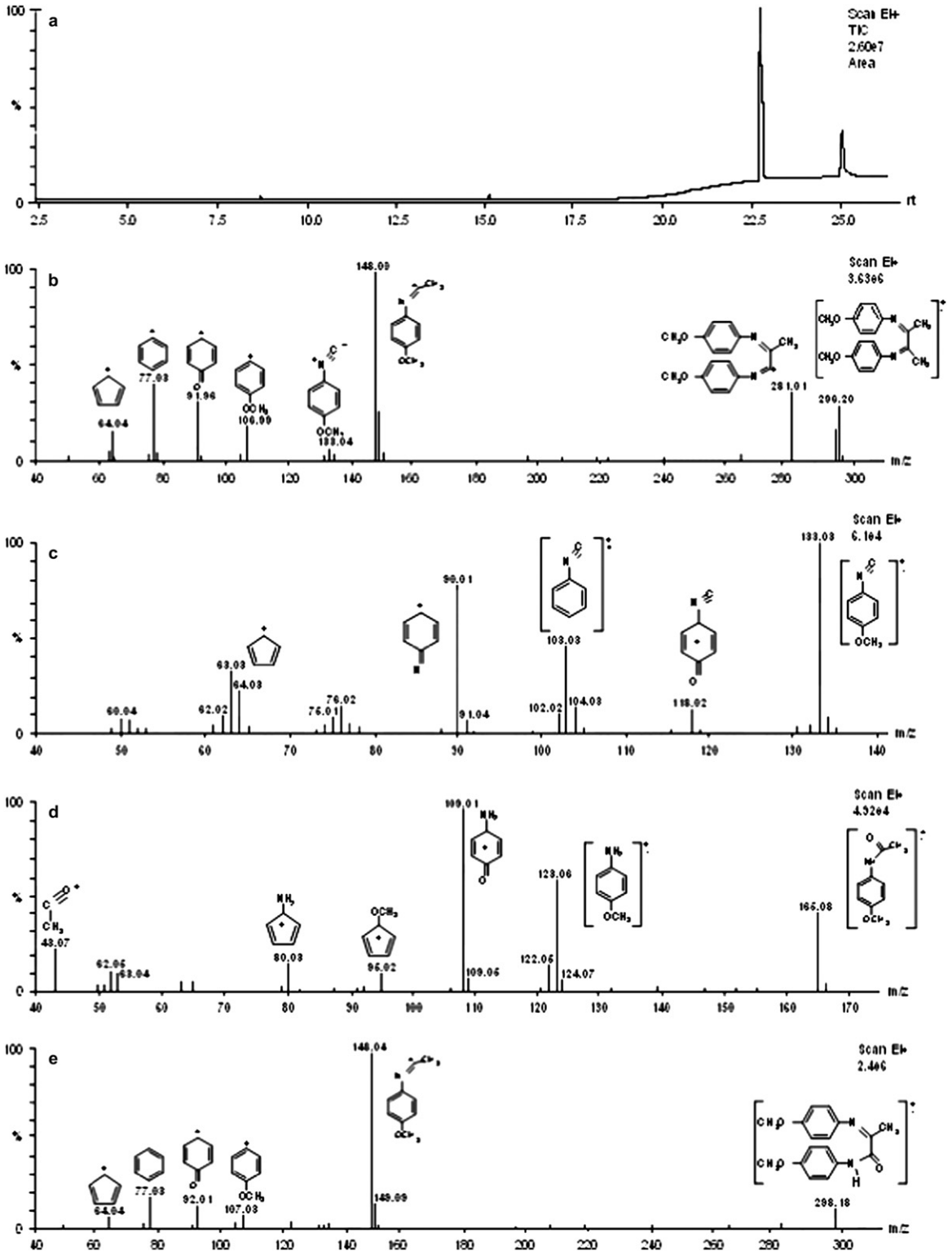

Figure 3. (a) GC–MS chromatogram of 1 mM 1,4-diaza-1,4-bis(*p*-methoxyphenyl)-2,3-dimethyl-1,3-butadiene (**11**) in benzene after 49 h of irradiation in the presence of TPP; (b) EI+ mass spectrum of **11**; (c) EI+ mass spectrum of compound with retention time 8.54 min; (d) EI+ mass spectrum of compound with retention time 15.22 min; (e) EI+ mass spectrum of compound with retention time 25.03 min.

(**15**) or addition of $O_2(^1\Delta_g)$ to the C═N double bond giving peroxaziridines (**16**) were disregarded on the basis of observed products.

Kinetic results obtained in this work indicate that k_T values for singlet oxygen quenching by dihydropyrazines are highly dependent on solvent properties (Table 1). A meaningful interpretation of k_T solvent dependence was obtained by using LSER solvatochromic equation. LSER correlations listed in Table 2 indicate that the singlet oxygen reaction with **5** has a different solvent dependence compared to that found for with other compounds. For **5**, the reaction rate

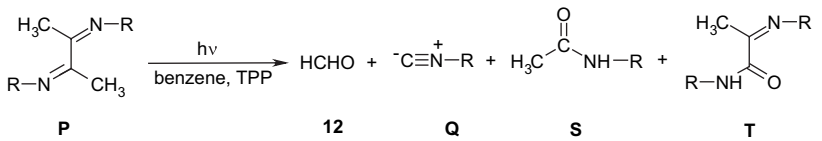

P 12 Q S T

R	P	Q	S	T
ϕ	10	10a	10b	10c
CH_3-O-ϕ	11	11a	11b	11c

Scheme 3.

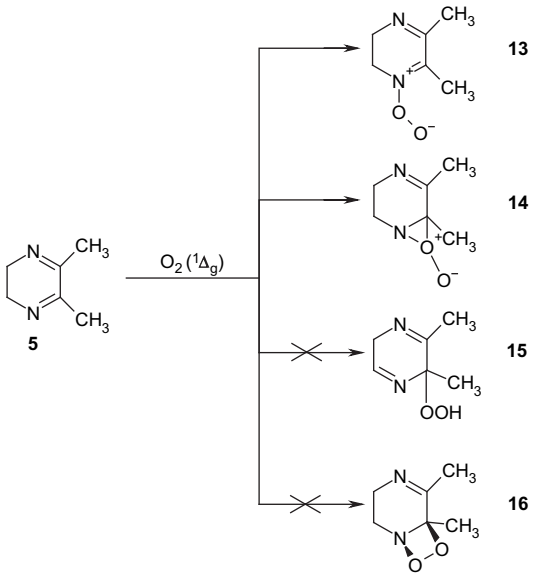

Scheme 4.

increases in solvents with higher capabilities to stabilize charges and dipoles, and decreases in strong hydrogen bond donor solvents. Data are compatible with an exciplex formation with considerable charge separation. This result could be in agreement with the formation of both perepoxide (**14**) and zwitterionic (**13**) intermediates as proposed by Gollnick et al.[27] Formation of these species as intermediates, in the ene reaction of singlet oxygen with alkenes, prior to the product determining step has been extensively discussed,[39–49] although recent theoretical studies predict two adjacent transition states without an intervening intermediate.[50]

Our results support the formation of a perepoxide as the primary intermediate arising from the interaction between singlet oxygen and **5**. The LSER equation for this compound shows that the relative statistical weight of the coefficient associated with the α parameter is smaller than the generally observed for electrophilic attack of singlet oxygen on a nitrogen lone pair in amino compounds. This result implies steric hindrance as a factor, likely due to hydrogen bonding between solvent and the nitrogen atom, inhibiting the reaction but not in the extent observed with tertiary amines.[2,17] This result could be understood if nitrogen is not the reactive centre but is close to it. In the same way, we also found that the coefficient associated with the π^* parameter is larger than that of reactions of $O_2(^1\Delta_g)$ with amines. Solvent dependence on k_R for reaction of **5** with $O_2(^1\Delta_g)$ is more significant than that observed for k_T. The chemical rate constant increases by more than 2 orders of magnitude when the solvent is changed from non-polar (e.g., hexane) to polar (e.g., propylencarbonate).[28] The contribution of the chemical reaction in non-polar solvents is negligible, whereas in highly polar solvents it represents the main deactivation channel. Solvent dependence of k_R can be explained if intermediates along the reaction coordinate have more localized charge than the initial complex. This result is compatible with involvement of ion pairs in controlling the final product distribution as depicted in Scheme 5.

The k_T value for reactions of **6** and **8** with singlet oxygen is substantially larger compared to **5**, in most solvents. The k_T value for **7** is comparable or slightly larger than that of **5**. Solvent effects for **6**, **7** and **8** analyzed in terms of LSER are characterized by Hildebrand parameter dependence of k_T. Dependence of rate constant on Hildebrand parameter has been ascribed to $O_2(^1\Delta_g)$ reactions, which involve a concerted or partially concerted cycloaddition of singlet oxygen to an activated diene.[11] The dependence on the Hildebrand parameter is explained in terms of formation of an encounter complex of smaller molecular volume compared to the parent compounds. Furthermore, these reactions are also affected by solvent dipolarity–polarizability. Moreover, examination of LSER equations for **6**, **7** and **8** shows that the reaction is also assisted by HBA and inhibited by HBD solvents. These results can be explained if phenyl substitution opens a further reactive channel in which the perepoxide is stabilized by interaction with the π system of a phenyl group.[28,51] A reaction mechanism compatible with our results is depicted in Scheme 6.

Reaction path (a), leads only to physical quenching through intersystem crossing to produce oxygen and the parent α-diimine. The geometry of the exciplex hinders intramolecular hydrogen abstraction processes more that it stabilizes it. Invoking the perepoxide structure (Scheme 6a) provides an explanation for the observed solvent dependence. Decrease of total reaction rate constants in HBD solvents can be understood in terms of interactions with the reactive centre (the phenyl substituted C=N double bond). Furthermore, the increase in sensitivity to HBA solvents may be due to electrostatic stabilizing interactions with a positive charge on the complex. In addition, dependence of k_T on the Hildebrand parameter can be understood in terms of a phenyl group–perepoxide interaction. This interaction would be favourable in solvents with high cohesive energy because interaction of negatively charged oxygen with the neighbouring phenyl disrupts solvent–phenyl group interactions in the substrate. In addition, this hypothesis permits us to explain the low values of the chemical reaction constant measured

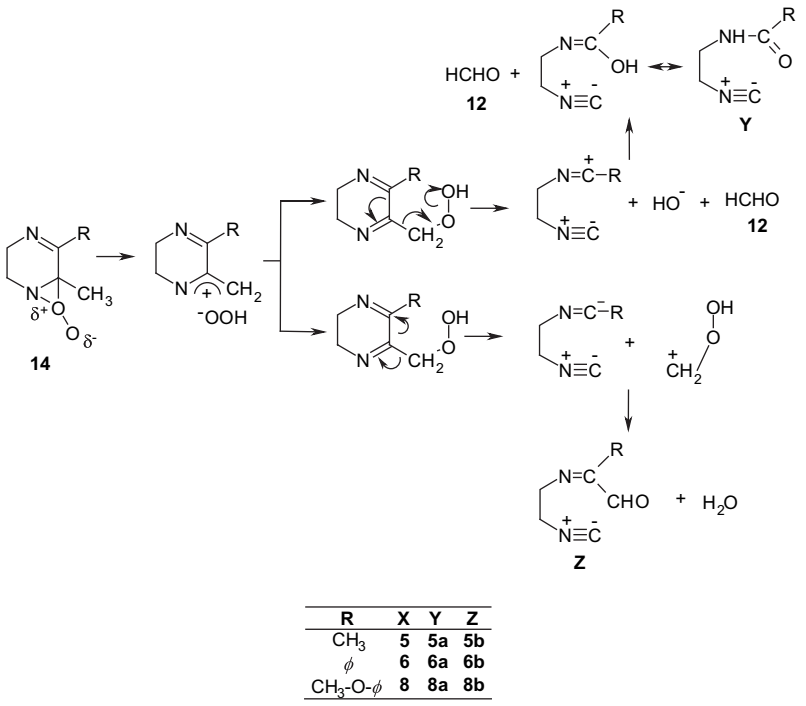

R	X	Y	Z
CH_3	5	5a	5b
ϕ	6	6a	6b
CH_3-O-ϕ	8	8a	8b

Scheme 5.

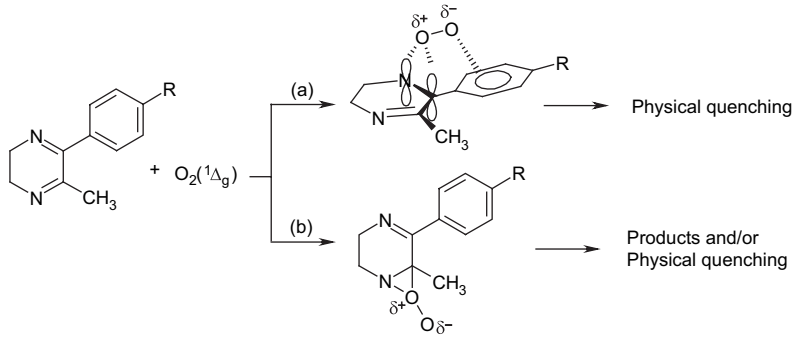

Scheme 6.

for **6** and **8** even in polar solvents and the absence of photooxidation products for **7** and **9**. As mentioned above, the only reaction products detected for **6** and **8** arise from singlet oxygen attack on a methyl substituted N–C double bond. The total reaction rate constant for **6** and **8** is larger than for the dimethyl substituted analogs. These data are consistent with the mechanism of sensitized photooxidation of **6** proposed in Scheme 6. The increased reactivity of **6** and **8** towards singlet oxygen, relative to the dimethyl substituted α-diimine (**5**), implies that the main path of reaction involves the interaction of $O_2(^1\Delta_g)$ with the phenyl substituted N–C double bond, to give a perepoxide-like exciplex that exclusively evolves by intersystem crossing since there is no any accessible α-hydrogen. Even though this mechanism would be the only path for reaction of singlet oxygen with **8**, this molecule is not much more reactive than **5**. This behaviour can be easily understood by considering results of restricted DFT_B3LYP/6-311G* molecular modelling. These calculations predict phenyl rings appreciably deviated from the coplanarity regarding the imino double bond. For **5** we found a dihedral angle of 39.7° between the phenyl and imino groups, while in the diphenyl substituted compound, **7**, the dihedral angle increases to 56.6°, due to the larger steric hindrance between the phenyl rings. If exciplex leading to physical quenching in Scheme 6 is considered, it can be noticed that a larger dihedral angle between the imino bond and the phenyl substituent would diminish the stabilizing interaction between the partially negative oxygen and the π system of the phenyl substituent, and consequently lower total rate constants would be expected. Compound **9** was the cyclic α-diimine that exhibits the smallest solvent effect. The LSER analysis for this compound shows that the reaction is assisted by HBA and inhibited by HBD solvents. This dependence on the microscopic solvent parameters was similar to that observed for **6**, **7** and **8** but k_T for **9** was found independent on the Hildebrand parameter. This behaviour can be explained by the effect of *p*-methoxyphenyl substituent. Important resonant electron donor effects cannot

be expected due to the lack of coplanarity among the imino and phenyl groups, on the contrary, the inductive electron acceptor effect would be predominant. This effect, more important for the methoxyphenyl group than the phenyl group,[39] diminishes the electron density on the imino bond and increases the negative charge on the phenyl ring π system, restricting both, the easiness of singlet oxygen electrophilic attack and the stabilizing interaction between the π system and the negative oxygen once the exciplex is formed. The effect permits us to explain the larger reactivity of **6** and **7** in comparison to the reactivity of **8** and **9**, respectively.

3.2. Acyclic α-diimines

Theoretical calculations predict a trans configuration of the two coplanar imino bonds as the most probable structure, with the phenyl substituents on the nitrogen slightly out of the plane due to steric interactions with methyl groups in positions 2 and 3. This configuration does not permit an eventual [2+4] cycloaddition of singlet oxygen to the conjugated double bonds. As mentioned above, the reactivity of acyclic α-diimines towards singlet oxygen is lower than that for the cyclic homologous by a factor 10–100, probably because of the most flexible linear structure. In addition, the data show k_T values strongly dependent on phenyl ring substituent, being more reactive than the *p*-methoxy substituted compound. The k_T values for **11** increase in solvents both with larger capacity to stabilize charges and dipoles, and with high cohesive energy. Also, they decrease in strong HBD solvents (Table 4). The dependence on the π^* parameter implies the formation of an exciplex with appreciable charge separation. Furthermore, the dependence on ρ_H^2 means a more compact exciplex than the parent compounds. This dependence is similar to that found for reaction of $O_2(^1\Delta_g)$ with 1,4-dimethylnaphthalene.[11] In this case, a partially concerted cycloaddition mechanism has been suggested to account for the dependence of the rate constant with solvent microscopic parameters. For **11** reaction with $O_2(^1\Delta_g)$, a partially concerted [2+2] cycloaddition, as shown in Scheme 7 is proposed to account for k_T dependence on the solvent. Decrease of k_T in HBD solvents can be explained in terms of interaction of acidic solvents with the nitrogen lone pair, which sterically hinders the access of excited oxygen to the reactive centre.

The lower reactivity of **10**, the reduced solvent effect on k_T and the dependence of k_T on the Hildebrand parameter in spite of the poor correlation can be interpreted based on two factors. First, the exciplex for this compound is formed through a concerted [2+2] cycloaddition with no charge separation, as shown in Scheme 7. Second, reactivity of acyclic α-diimines is dependent on resonant effects of *p*-substituent in the phenyl group. The large resonant electron donor capacity of *p*-methoxy substituent in **11** increases the reactivity of this compound relative to the non-substituted **10**.

A concerted or partially concerted cycloaddition reaction mode would allow us to rationalize product distribution over extended periods of time in photooxidation experiments and similarly explain the dependence on solvent polarity. Identical product distributions are found in polar and non-polar solvents, but their relative concentrations change according to the media. This implies that at least two different intermediates lead to the detected products. The first intermediate may be highly favoured in polar solvents because of larger k_R values in these solvents. The intermediate could then rearrange to a non-polar intermediate in non-polar solvents. Scheme 8 shows a mechanism explaining these results.

In Scheme 8, path (a) accounts for 1-isocyano-4-methoxybenzene (**11a**) and *N*-(4-methoxyphenyl)acetamide (**11b**), the main products observed in the photooxygenation of **11** in propylencarbonate. Path (b) explains the smaller reactivity in benzene as solvent and the increase in *N*-phenyl-2-(phenylimino)propanamide (**11c**) relative concentration. A similar mechanism has been proposed by Ito et al.[23] to explain product distribution in sensitized oxidation of hydrazones.

3.3. Conclusions

The 5,6-disubstituted cyclic α-diimines are moderate to efficient singlet oxygen quenchers, and are most effective in polar solvents. A reaction mechanism involving a perepoxide intermediate that forms a hydroperoxide appears to be the main reaction path from which the products arise. The replacement of a phenyl substituent with a methyl substituent opens an additional reaction path involving a perepoxide-like exciplex in which a stabilizing interaction of the negative charge on the free oxygen of a perepoxide with aromatic π system contributes to an increased singlet oxygen quenching ability of cyclic α-diimines. 1,4-Disubstituted acyclic α-diimines are moderate to poor singlet oxygen quenchers. The total rate constants are scarcely dependent on the solvent properties. A reaction mechanism involving a dioxetane-like exciplex that evolves to a charged intermediate from which products are formed is most likely the main reaction path in polar solvents.

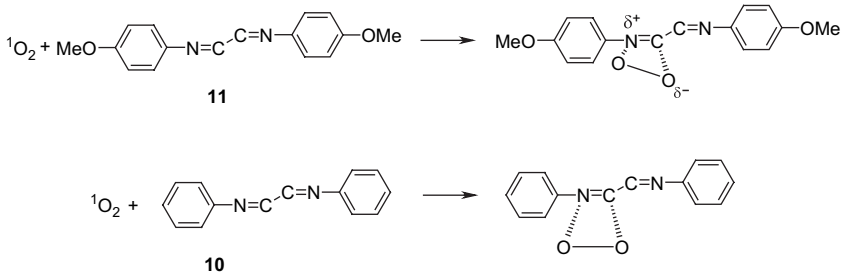

Scheme 7.

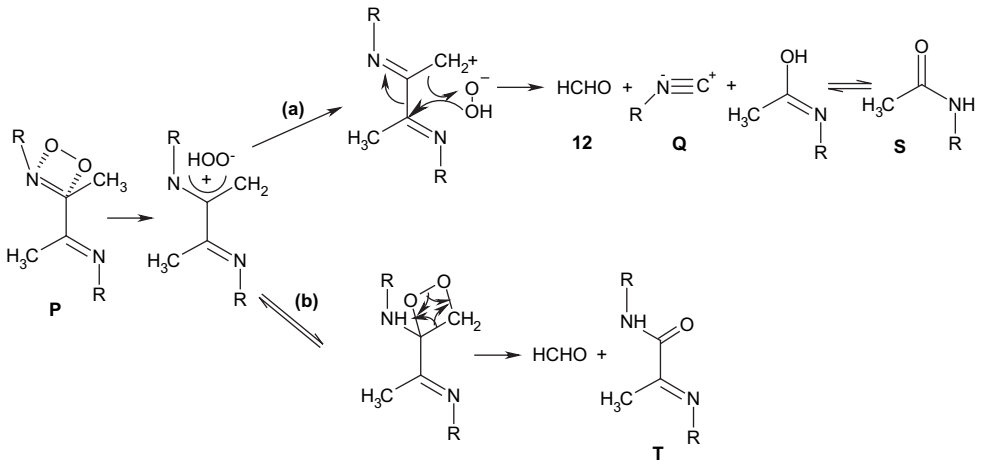

R	P	Q	S	T
ϕ	10	10a	10b	10c
CH_3O-ϕ	11	11a	11b	11c

Scheme 8.

4. Experimental

4.1. General

Melting points (not corrected) were determined employing both a modified Koffler and a Electrothermal 9200 apparatus. NMR spectra were obtained from a Bruker DRX-300 spectrometer. Chemical shifts are referred to internal tetramethylsilane, TMS. Elemental analyses were performed on a Fisons EA 1108 instrument. IR spectra were obtained on a Fourier transform Bruker IFS-56 spectrometer. UV–vis measurements were made in a Unicam UV-4 spectrophotometer. A Fisons MD-800 GC–MS system with a Hewlett Packard Ultra-2 capillary column (25 m) was used to obtain electron impact mass spectra. All spectroscopic measurements were performed at room temperature.

4.2. Materials

All solvents used in the synthesis were of reagent grade. In spectroscopic and kinetic measurements, spectroscopic or HPLC quality solvents were used. 5,10,15,20-Tetraphenyl-21*H*,23*H*-porphine (TPP), 99%, and 9,10-dimethyl-anthracene, (DMA), 99%, from Aldrich were used without further purification. Rose Bengal (RB), 96%, from Fluka, was recrystallized twice from ethanol prior to use.

4.3. Methods

Chemical reaction rate constants were determined in several selected solvents using a 10 ml double wall cell, light-protected by black paint. A centred window allowed irradiation with light of a given wavelength using *Schott* cut-off filters. Circulating water maintained the cell temperature at 22±0.5 °C. Sensitizer irradiation, RB or TPP was performed with a visible, 200 W, Par lamp. A *Hewlett Packard 5890* gas chromatograph equipped with a NPD detector and a *Hewlett Packard Ultra-2* capillary column was used to monitor substrate consumption. In a typical run, 0.001 M substrate solution was irradiated in the presence of the sensitizer up to ∼30 to 40% conversion. At least six duplicate 50 μL samples at different time intervals were taken for GC analysis. DMA was used as actinometer.

Time-resolved luminescence measurements were carried out in 1 cm path fluorescence cells. TPP or RB were excited by the second harmonic (532 nm, ca. 9 mJ per pulse) of 6-ns light pulse of a *Quantel Brilliant* Q-Switched Nd:YAG laser. A liquid-nitrogen cooled North *Coast model EO-817P* germanium photodiode detector with a built-in preamplifier was used to detect infrared radiation from the cell. Detector was coupled to the cell at right angle. An interference filter (1270 nm, *Spectrogon US, Inc*.) and a cut-off filter (995 nm, *Andover Corp*.) were the only elements between cell face and the diode cover plate. Preamplifier output was fed into the 1 MΩ input of a digitizing oscilloscope *Hewlett Packard model 54540 A*. Computerized experiment control, data acquisition and analysis were performed with a LabView based software developed in our laboratory.

Restricted density functional theory calculations were made using Gaussian 03W software. All structures were geometry optimized at the B3LYP/6-311G* level.

Equation coefficients and statistical parameters of LSER and TLSER correlations were obtained by multilinear correlation analysis with STAT VIEW 5.0 (SAS Institute Inc.). Results agreed with the *t*-statistic of descriptors.

4.4. Chemical synthesis

4.4.1. Synthesis of cyclic α-diimines. 5,6-Disubstituted-2,3-dihydropyrazines were synthesized as previously described.[52] Typically, a solution of the corresponding diketone (5 g) in ethyl ether (10 ml) was added to ethylendiamine (2 g) in 10 ml of ethyl ether maintained at 0 °C. The mixture was refluxed for 30 min and the ethereal solution

was dried over sodium sulfate and solvent removed in vacuum. The remaining oil was cooled in a freezer during several hours producing a solid from which pure 5,6-disubstituted-2,3-dihydropyrazine was obtained as yellow needles by recrystallization from ethyl ether–hexane.

4.4.1.1. 5-Methyl-6-phenyl-2,3-dihydropyrazine (6). This compound was prepared in 50% yield from 1-phenyl-1,2-propanedione according to the already described procedure; mp 34–37 °C (lit.[27,53] mp 38–39 °C). ^{1}H NMR ($CDCl_3$): δ 2.1 ppm (s, 3H), 3.35–3.55 ppm (m, 4H), 7.3–7.4 (m, 5H). IR (KBr, ν, cm^{-1}): 2944, 2833, 1636, 1569, 1440. MS m/e=172 (M^+), 157, 131, 103, 77.

4.4.1.2. 5,6-Dimethyl-2,3-dihydropyrazine (5). Following the procedure for the preparation of MPD, the condensation reaction between ethylendiamine and 2,3-butanedione afforded a liquid reaction crude. Careful distillation under nitrogen was required to obtain pure DMD, yield 40%, bp 58 °C (15 mmHg) (lit.[52,53] bp 53–54 °C (12 Torr), 60–62 °C (18 Torr)). ^{1}H NMR ($CDCl_3$): δ 1.87 ppm (s, 6H), 3.07 ppm (s, 4H). IR (KBr, ν, cm^{-1}): 2949, 2845, 1655, 1598, 1439. MS m/e=110 (M^+), 95, 69, 54, 42.

4.4.1.3. 5,6-Diphenyl-2,3-dihydropyrazine (7). In a reaction similar to that of DMD, 4.2 g (20 mmol) of benzyl and 1.2 g (20 mmol) of ethylendiamine yields 85% of DPD; mp 163–165 °C (lit.[27,53] mp 162.5–163.5 °C). ^{1}H NMR (CDCl): δ 3.72 ppm (s, 4H), 7.26–7.43 ppm (m, 10H). IR (KBr, ν, cm^{-1}): 2942, 2831, 1553, 1490. MS m/e=234 (M^+), 176, 131, 103, 77.

4.4.1.4. 5,6-Bis(*p*-methoxyphenyl)-2,3-dihydropyrazine (9). Following the same procedure to synthesize DMD 2.2 g (8.3 mmol) of 4,4′-dimethoxybenzyl and 0.5 g (8.3 mmol) of ethylendiamine afforded a pale yellow solid, after purification by employing a chromatographic column packed with silica and chloroform as the eluent. Subsequent recrystallization from ethanol yield 75% of pure BMPD; mp 127–129 °C with dec. ^{1}H NMR ($CDCl_3$): δ 3.56 ppm (s, 4H), 3.71 ppm (s, 6H), 6.76–7.38 ppm (m, 8H). IR (KBr, ν, cm^{-1}): 2938, 2835, 1633, 1441. MS m/e=294 (M^+), 263, 133, 103, 77. Elem. anal. calcd %C: 73.47, %H: 6.12, %N: 9.52; exp. %C: 73.26, %H: 6.17, %N: 9.78.

4.4.1.5. 5-Methyl-6-(*p*-methoxyphenyl)-2,3-dihydropyrazine (8). This compound was prepared in 75% yield from 0.5 g (2.7 mmol) of 1-(*p*-methoxyphenyl)-1,2-propanedione according to the already described procedure. ^{1}H NMR ($CDCl_3$): δ 2.05 ppm (s, 3H), 3.38–3.48 ppm (m, 4H), 3.77 ppm (s, 3H), 6.86 ppm (d, 2H), 7.37 ppm (d, 2H). IR (KBr, ν, cm^{-1}): 2940, 2837, 1581, 1512, 1439 cm^{-1}. MS m/e=202 (M^+), 171, 133, 103, 77. Elem. anal. calcd %C: 71.26, %H: 6.98, %N: 13.85; exp. %C: 71.06, %H: 7.04, %N: 14.23.

4.4.2. Synthesis of acyclic α-diimines. Acyclic α-diimines were synthesized through the condensation reaction of aromatic amines with 2,3-butanedione.[54] Typically, a solution of the corresponding aromatic amine (5 g) in 10 ml of ethanol was added to butanedione (2 g) in 5 ml of ethanol. The mixture was gently warmed for 30 min and stirred at room temperature for 24 h to obtain a crystalline yellow solid. The solid was filtered, washed with cold ethanol and recrystallized from ethanol to obtain the pure product.

4.4.2.1. 1,4-Diaza-1,4-diphenyl-2,3-dimethyl-1,3-butadiene (10). This compound was prepared in 49% yield from aniline according to the already described procedure; mp 137–139 °C (lit.[54] mp 136–137 °C). ^{1}H NMR ($CDCl_3$): δ 2.15 ppm (s, 6H), 6.77–6.81 ppm (m, 2H), 7.08–7.14 ppm (m, 1H), 7.33–7.40 ppm (m, 2H). IR (KBr, ν, cm^{-1}): 3058, 1634, 1590, 1480, 1445. MS m/e=236 (M^+), 118, 103, 77, 51. Elem. anal. calcd %C: 81.35, %H: 6.78, %N: 11.86; exp. %C: 81.14, %H: 7.02, %N: 12.22.

4.4.2.2. 1,4-Diaza-1,4-bis(*p*-methoxyphenyl)-2,3-dimethyl-1,3-butadiene (11). In a reaction similar to that of DPDM, 3.8 g (31 mmol) of *p*-anisidine and 1.2 g (14 mmol) of 2,3-butanedione yields 52% of DMPDM; mp 185–186 °C. ^{1}H NMR ($CDCl_3$): δ 2.18 ppm (s, 6H), 3.82 ppm (s, 6H), 6.78 ppm (d, 2H), 6.91 ppm (d, 2H). IR (KBr, ν, cm^{-1}): 2960, 1633, 1501, 1469. MS m/e=296 (M^+), 281, 148, 92, 77. Elem. anal. calcd %C: 72.97, %H: 6.76, %N: 9.46; exp. %C: 72.67, %H: 7.01, %N: 9.48.

Acknowledgements

Financial support from FONDECYT (grant 2990096) and Departamento de Postgrado de la Universidad de Chile (grants PG/037/98 and PG/51/99) are gratefully acknowledged.

References and notes

1. Wilkinson, F.; Brummer, J. G. *J. Phys. Chem. Ref. Data* **1981**, *10*, 809–899; Wilkinson, F.; Helman, W. P.; Ross, A. B. http://allen.rad.nd.edu/compilations/SingOx.
2. Lissi, E. A.; Encinas, M. V.; Lemp, E.; Rubio, M. A. *Chem. Rev.* **1993**, *93*, 699–723.
3. Lissi, E. A.; Rubio, M. A. *Pure Appl. Chem.* **1990**, *62*, 1503–1510.
4. Lissi, E. A.; Lemp, E.; Zanocco, A. L. *Understanding and Manipulating Excited-state Processes*; Ramamurthy, V., Schanze, K. S., Eds.; Marcel Dekker: New York, NY, 2001; Vol. 4, pp 287–316.
5. Lemp, E.; Zanocco, A. L.; Lissi, E. A. *Curr. Org. Chem.* **2003**, *7*, 799–819.
6. Schweitzer, C.; Schmidt, R. *Chem. Rev.* **2003**, *103*, 1685–1757.
7. Palumbo, M. C.; García, N. A.; Arguello, G. A. *J. Photochem. Photobiol. B, Biol.* **1990**, *7*, 33–42.
8. Mandard-Cazin, B.; Aubry, J.-M.; Rigaudy, J. *J. Chem. Soc., Chem. Commun.* **1986**, 952–953.
9. Gollnick, K.; Griesbeck, A. *Tetrahedron Lett.* **1984**, *25*, 725–728.
10. Mártire, D. O.; Braslavsky, S. E.; García, N. A. *J. Photochem. Photobiol. A, Chem.* **1991**, *61*, 113–124.
11. Aubry, J.-M.; Mandard-Cazin, B.; Rougee, M.; Bensasson, R. V. *J. Am. Chem. Soc.* **1995**, *117*, 9159–9164.
12. Encinas, M. V.; Lemp, E.; Lissi, E. A. *J. Chem. Soc., Perkin Trans. 2* **1987**, 1125–1127.
13. Clennan, E. L.; Noe, L. J.; Wen, T.; Szneler, E. *J. Org. Chem.* **1989**, *54*, 3581–3584.
14. Zanocco, A. L.; Günther, G.; Lemp, E.; De la Fuente, J. R.; Pizarro, N. *J. Photochem. Photobiol. A, Chem.* **2001**, *140*, 109–115.

15. Darmanyan, A. P.; Jenksh, W. S. *J. Phys. Chem. A* **1998**, *102*, 7420–7426.
16. Catalan, J.; Diaz, C.; Barrio, L. *Chem. Phys.* **2004**, *300*, 33–39.
17. Zanocco, A. L.; Günther, G.; Lemp, E.; de la Fuente, J. R.; Pizarro, N. *Photochem. Photobiol.* **1998**, *68*, 487–493.
18. Zanocco, A. L.; Lemp, E.; Günther, G. *J. Chem. Soc., Perkin Trans. 2* **1997**, 1299–1302.
19. Lemp, E.; Gunther, G.; Castro, R.; Curitol, M.; Zanocco, A. L. *J. Photochem. Photobiol. A, Chem.* **2005**, *175*, 146–153.
20. Lemp, E.; Pizarro, N.; Encinas, M. V.; Zanocco, A. L. *Phys. Chem. Chem. Phys.* **2001**, *3*, 5222–5225.
21. Lemp, E.; Valencia, C.; Zanocco, A. L. *J. Photochem. Photobiol. A, Chem.* **2004**, *168*, 91–96.
22. George, M. V.; Bhat, V. *Chem. Rev.* **1979**, *79*, 447–478.
23. Ito, Y.; Kyono, K.; Matsuura, T. *Tetrahedron Lett.* **1979**, 2253–2256.
24. Vaidya, V. K. *J. Photochem. Photobiol. A, Chem.* **1994**, *81*, 135–137.
25. Castro, C.; Dixon, M.; Erden, I.; Ergonec, P.; Keeffe, J.; Sukhovistsky, A. *J. Org. Chem.* **1989**, *54*, 3732–3738.
26. Erden, I.; Griffin, A.; Keeffe, J.; Brinck-Kohn, V. *Tetrahedron Lett.* **1993**, *34*, 793–796.
27. Gollnick, K.; Koegler, S.; Maurer, D. *J. Org. Chem.* **1992**, *57*, 229–234.
28. Lemp, E.; Zanocco, A. L.; Günther, G.; Pizarro, N. *J. Org. Chem.* **2003**, *68*, 3009–3016.
29. Reichardt, C. *Solvents and Solvent Effects in Organic Chemistry*, 2nd ed.; VCH: Weinheim, 1990.
30. Kamlet, M. J.; Abboud, J. L. M.; Abraham, M. H.; Taft, R. W. *J. Org. Chem.* **1983**, *48*, 2877–2887.
31. Abraham, M. H.; Doherty, R. M.; Kamlet, M. J.; Harris, J. M.; Taft, R. W. *J. Chem. Soc., Perkin Trans. 2* **1987**, 913–920.
32. Carlson, D. J.; Mendenhall, E. D.; Suprunchuk, T.; Wiles, D. M. *J. Am. Chem. Soc.* **1972**, *94*, 8960–8963.
33. Michaeli, A.; Feitelson, J. *Photochem. Photobiol.* **1994**, *59*, 284–288.
34. Kamlet, M. J.; Carr, P. W.; Taft, R. W.; Abraham, M. H. *J. Am. Chem. Soc.* **1981**, *103*, 6062–6066.
35. Barton, A. F. M. *Chem. Rev.* **1975**, *75*, 731–752.
36. Belsley, D. A.; Kuh, E.; Welsch, R. E. *Regression Diagnostics. Identifying Influential Data and Sources of Collinearity*; Wiley: New York, NY, 1980.
37. Gunther, G.; Lemp, E.; Zanocco, A. L. *Bol. Soc. Chil. Quim.* **2000**, *45*, 637–644.
38. Pretsch, E.; Bühlmann, P.; Affolter, C.; Herrera, A.; Martínez, R. *Determinación Estructural de Compuestos Orgánicos*; Springer: Barcelona, 2001.
39. Stratakis, M.; Orfanopoulos, M.; Foote, C. S. *J. Org. Chem.* **1998**, *63*, 1315–1318.
40. Jefford, C. W.; Rimbault, C. G. *J. Am. Chem. Soc.* **1978**, *100*, 295–296.
41. Jefford, C. W.; Rimbault, C. G. *J. Am. Chem. Soc.* **1978**, *100*, 6437–6445.
42. Manring, L. E.; Foote, C. S. *J. Am. Chem. Soc.* **1983**, *105*, 4710–4717.
43. Wilson, S. L.; Schuster, G. B. *J. Org. Chem.* **1986**, *51*, 2056–2060.
44. Fenical, W.; Kearns, D. R.; Radlick, P. *J. Am. Chem. Soc.* **1969**, *91*, 3396–3398.
45. Frimer, A. A.; Bartlett, P. D.; Boschung, A. F.; Jewett, J. G. *J. Am. Chem. Soc.* **1977**, *99*, 7977–7986.
46. Poon, T. H. W.; Pringle, K.; Foote, C. S. *J. Am. Chem. Soc.* **1995**, *117*, 7611–7618.
47. Stratakis, M.; Orfanopoulos, M.; Foote, C. S. *J. Am. Chem. Soc.* **1991**, *32*, 863–866.
48. Orfanopoulos, M.; Stephenson, L. M. *J. Am. Chem. Soc.* **1980**, *102*, 1417–1418.
49. Grdina, B.; Orfanopoulos, M.; Stephenson, L. M. *J. Am. Chem. Soc.* **1979**, *101*, 3111–3112.
50. Singleton, D. A.; Hang, Ch.; Szymanski, M. J.; Meyer, M. P.; Leach, A. G.; Kuwata, K. T.; Chen, J. S.; Greer, A.; Foote, C. S.; Houk, K. N. *J. Am. Chem. Soc.* **2003**, *125*, 1319–1328.
51. Stratakis, M.; Orfanopoulus, M. *Tetrahedron* **2000**, *56*, 1595–1615.
52. Flamet, I. F.; Stoll, M. *Helv. Chim. Acta* **1967**, *50*, 1754–1758.
53. Beak, P.; Miesel, J. L. *J. Am. Chem. Soc.* **1967**, *80*, 2375–2384.
54. Ferguson, L.; Goodwin, T. *J. Am. Chem. Soc.* **1949**, *71*, 633–637.